Article

Interaction of *Jania rubens* Polyphenolic Extract as an Antidiabetic Agent with α-Amylase, Lipase, and Trypsin: In Vitro Evaluations and In Silico Studies

Asmaa Nabil-Adam [1,*], Mohamed L. Ashour [2,3], Tamer M. Tamer [4], Mohamed A. Shreadah [1] and Mohamed A. Hassan [5,6,*]

[1] Marine Biotechnology and Natural Products Laboratory, National Institute of Oceanography & Fisheries, Cairo 11516, Egypt

[2] Department of Pharmacognosy, Faculty of Pharmacy, Ain-Shams University, Abbasia, Cairo 11566, Egypt

[3] Department of Pharmaceutical Sciences, Pharmacy Program, Batterjee Medical College, P.O. Box 6231, Jeddah 21442, Saudi Arabia

[4] Polymer Materials Research Department, Advanced Technologies and New Materials Research Institute (ATNMRI), City of Scientific Research and Technological Applications (SRTA-City), New Borg El-Arab City 21934, Alexandria, Egypt

[5] Protein Research Department, Genetic Engineering and Biotechnology Research Institute (GEBRI), City of Scientific Research and Technological Applications (SRTA-City), New Borg El-Arab City 21934, Alexandria, Egypt

[6] University Medical Center Göttingen, Georg-August-University, 37073 Göttingen, Germany

* Correspondence: sama.biomarine@gmail.com (A.N.-A.); madel@srtacity.sci.eg (M.A.H.)

Abstract: *Jania rubens* red seaweed has various bioactive compounds that can be used for several medicinal and pharmaceutical applications. In this study, we investigate the antidiabetic, anti-inflammatory, and antioxidant competency of *Jania rubens* polyphenolic extract (JRPE) by assessing their interactions with α-amylase, lipase, and trypsin enzymes. HPLC analysis revealed the dominance of twelve polyphenolic compounds. We performed computational analysis using α-amylase, lipase, and trypsin as target proteins for the polyphenols to explore their activities based on their predicted modes of binding sites following molecular modeling analysis. The molecular docking analysis demonstrated a good affinity score with a noticeable affinity to polyphenolic compositions of *Jania rubens*. The compounds with the highest affinity score for α-amylase (PDB: 4W93) were kaempferol, quercetin, and chlorogenic acid, with −8.4, −8.8 and −8 kcal/mol, respectively. Similarly, lipase (PDB: 1LPB) demonstrated high docking scores of −7.1, −7.4, and −7.2 kcal/mol for kaempferol, quercetin, and chlorogenic acid, respectively. Furthermore, for trypsin (PDB: 4DOQ) results, kaempferol, quercetin, and chlorogenic acid docking scores were −7.2, −7.2, and −7.1 kcal/mol, respectively. The docking findings were verified using in vitro evaluations, manifesting comparable results. Overall, these findings enlighten that the JRPE has antidiabetic, anti-inflammatory, and antioxidant properties using different diabetics' enzymes that could be further studied using in vivo investigations for diabetes treatment.

Keywords: *Jania rubens*; α-amylase; lipase; trypsin; antidiabetic; in silico analysis

1. Introduction

Obesity and diabetes (diabetes mellitus, DM) instigate several chronic diseases, including cardiovascular disease, kidney disease, eye disease, hypertension, osteoarthritis, and some forms of cancer. The worldwide rise of these conditions has become a major health concern. Excess fat mass accumulation is the defining feature of obesity, a complicated metabolic condition often accompanied by insulin resistance, elevated oxidative stress, and low-grade inflammation. Diabetes is a metabolic disorder caused by either a lack of pancreatic beta cells or a deficiency in insulin secretion and performance in terms of insulin

resistance and sensitivity with different cell types. Genetic predisposition, a Western-style fast food diet, insufficient exercise, and socioeconomic standing are all thought to play a role in the epidemic of obesity. More than 600 million adults are overweight or obese, and an alarmingly rising percentage of infants are born overweight or obese in developing nations, according to research by the International Obesity Task Force.

By 2045, it is projected that 629 million people will have diabetes, up from 425 million in 2017. More than 85% of the diagnosed cases of diabetes were type 2 diabetes. Vascular diseases such as nephropathy, retinopathy, peripheral neuropathy, and stroke were present in many diabetic patients [1]. According to the International Diabetes Federation's (IDF) ninth-edition report on global diabetes (2019), the worldwide prevalence of diabetes was 9.3%, and approximately 463 million people were affected by diabetes worldwide (International Diabetes Federation 2019) [2]. Another study looking at the global prevalence of overweight and obesity between 1980 and 2015 found that, while the rate of obesity was highest in disadvantaged groups in high-income countries, it was highest in wealthy and urban families in low-income countries. The rapid changes in socioeconomic status and the acceptance of high-calorie, fat-rich foods and less active lifestyles have led to a considerable increase in obesity rates worldwide [3].

Obesity is currently treated with a variety of conventional medications; for instance, sibutramine (Meridia) and lorcaserin (Belviq). Despite their effectiveness, these drugs are rarely used due to concerns about their accessibility and safety. Moreover, recent studies reported the synthesis of new compounds to inhibit glycosidase enzymes implicated in various biomedical applications [4,5]. However, it is important to create accessible entities that are also secure, efficient, and cheap to use. It is widely accepted that medicines derived from plants should be used as the first line of defense in preventing illness and its complications [6,7]. Traditional synthetics have consistently provided a rich vein of novel chemical compounds from which to extract useful pharmaceuticals. Phytogenic herbal products account for over half of all FDA-approved prescriptions. Proteins, minerals, and vitamins can all be abundant in seaweeds, as can dietary fiber (non-starch polysaccharides) due to their low lipid content and reduced caloric value, as well as the fact that they disrupt increasing the other nutrients in your diet's bioavailability [8]. In addition, the dietary fiber found in seaweeds comes mostly from polysaccharides, including alginates, cellulose, fucans, and laminarins, all of which are indigestible to humans due to a lack of certain enzymes.

Marine biotechnology (also called blue biotechnology) involves the application of biological resources from the sea for industrial, medical, or environmental purposes [9–11]. On the other hand, enzymes are the dominant molecular targets for the major medicinal molecules introduced to the market. Moreover, they are considered a favorable target for new drug discovery due to their protein structures, which facilitate the exploration of diverse drugs with potential target validation. Clinical applications of enzyme inhibitors have suggested new avenues for enzyme implementation in various medical fields, including oncology, cardiology, diabetes, and neurology [12–14]. Trypsin and α-amylase inhibitors play vital roles in diabetes management since they hinder the digestion of dietary carbohydrates, reducing the risk of postprandial hyperglycemia [15,16]. Additionally, lipase enzymes are widely exploited in various biotechnological applications [17]. Importantly, carbohydrate and pancreatic lipase inhibition effectively impede weight gain and treat obesity through calorie restrictions [18,19]. Therefore, α-amylase, lipase, and trypsin inhibition assays are broadly applied in the screening of different plant extracts and natural products as a typical approach to the development of novel antidiabetic and anti-obesity medications. Polyphenols are one of the key plant compounds that have been demonstrated to possess considerable biomedical activity, such as their application in preventing cancer and heart disease and their significant role as natural antioxidants in the food industry.

Green algae (*Chlorophyta*), red algae (*Rhodophyta*), and brown algae (*Phaeophyta*) are the three main types of marine macroalgae based on their pigmentation [20,21]. Chemically speaking, macroalgae are characterized by a high percentage of water, carbohydrates, and

proteins in addition to a low amount of lipids [22]. Rhodophyta, the red algae phylum, has the highest concentration of bioactive compounds, with over 1600 unique compounds accounting for 53% of all bioactive compounds found in algae [23]. Therefore, the current study investigates the biomedical application of the polyphenolic extract from Egyptian red algae (*Jania rubens*), JRPE, for the first time using different in vitro approaches, including antioxidant, anti-inflammatory, and antibacterial evaluations. Furthermore, the antidiabetic property of the JRPE was appraised through investigation for its ability to inhibit the pancreatic enzymes activity, such as α-amylase, lipase, and trypsin. Moreover, in silico computational drug screening studies were performed against these enzymes responsible for obesity and diabetes, which are targets for anti-diabetes treatment.

2. Results

2.1. The HPLC Analysis of JRPE

The HPLC analysis results of *Jania rubens* polyphenolic extract (JRPE) exhibited high concentrations of polyphenolic compositions, revealing the presence of 12 compounds, as depicted in Figure S1. Figure 1 illustrates the chemical structures of the identified polyphenolic compounds. It can be observed from the data in Table 1 that kaempferol, resveratrol, quercetin, and syringic acid are dominant products at concentrations of 140.68, 96.88, 67.48, and 49.60 mg/kg, respectively. In terms of the ratio of the polyphenolic compounds in JRPE, kaempferol revealed the highest percentage of 32.5%, followed by resveratrol (22%), quercetin (15%), syringic acid (11%), ferulic acid (6%), *o*-coumaric, vanillic, and caffeic acid (2%), while *p*-coumaric acid had the lowest concentration.

Table 1. Concentrations of polyphenolic compounds in JRPE based on HPLC analysis.

Polyphenolic Compounds	R. T/min	Con. (mg/kg)
p-Hydroxybenzoic acid	7.618	14.61616
Caffeic acid	9.954	6.93052
Catechin	9.124	3.99015
Chlorogenic	9.408	17.91833
Ferulic acid	15.715	25.81511
Kaempferol	24.757	140.68073
o-Coumaric acid	17.874	8.01992
p-Coumaric acid	13.526	1.71484
Quercetin	21.666	67.48636
Resveratrol	19.470	96.88487
Syringic acid	10.705	49.60852
Vanillic acid	15.40824	7.13708

2.2. The Antioxidant Properties of the JRPE

Figure 2A depicts the total antioxidant capacity (TAC) of JRPE in the presence of VitC as a reference, demonstrating that the TAC for JRPE is greater than VitC at all concentrations tested. However, the VitC demonstrated a slight increase in TAC compared to the JRPE at a concentration of 1000 μg/mL. In addition, the IC50 of TAC for JRE is 253.43 μg/mL, which is equivalent to VitC.

The antioxidant activity of the JRPE using DPPH methods compared with VitC as the standard antioxidant natural material revealed that JRPE had higher activity at concentrations from 300 to 700 μg/mL compared to VitC. Nevertheless, comparable antioxidant capacities for the JRPE and VitC were perceived at concentrations of 900 μg/mL and 1000 μg/mL. These findings substantiate those obtained from TAC. Furthermore, the IC50 values for the JRPE and VitC were 3.8772 μg/mL and 5601 μg/mL, respectively, as demonstrated in Figure 2B.
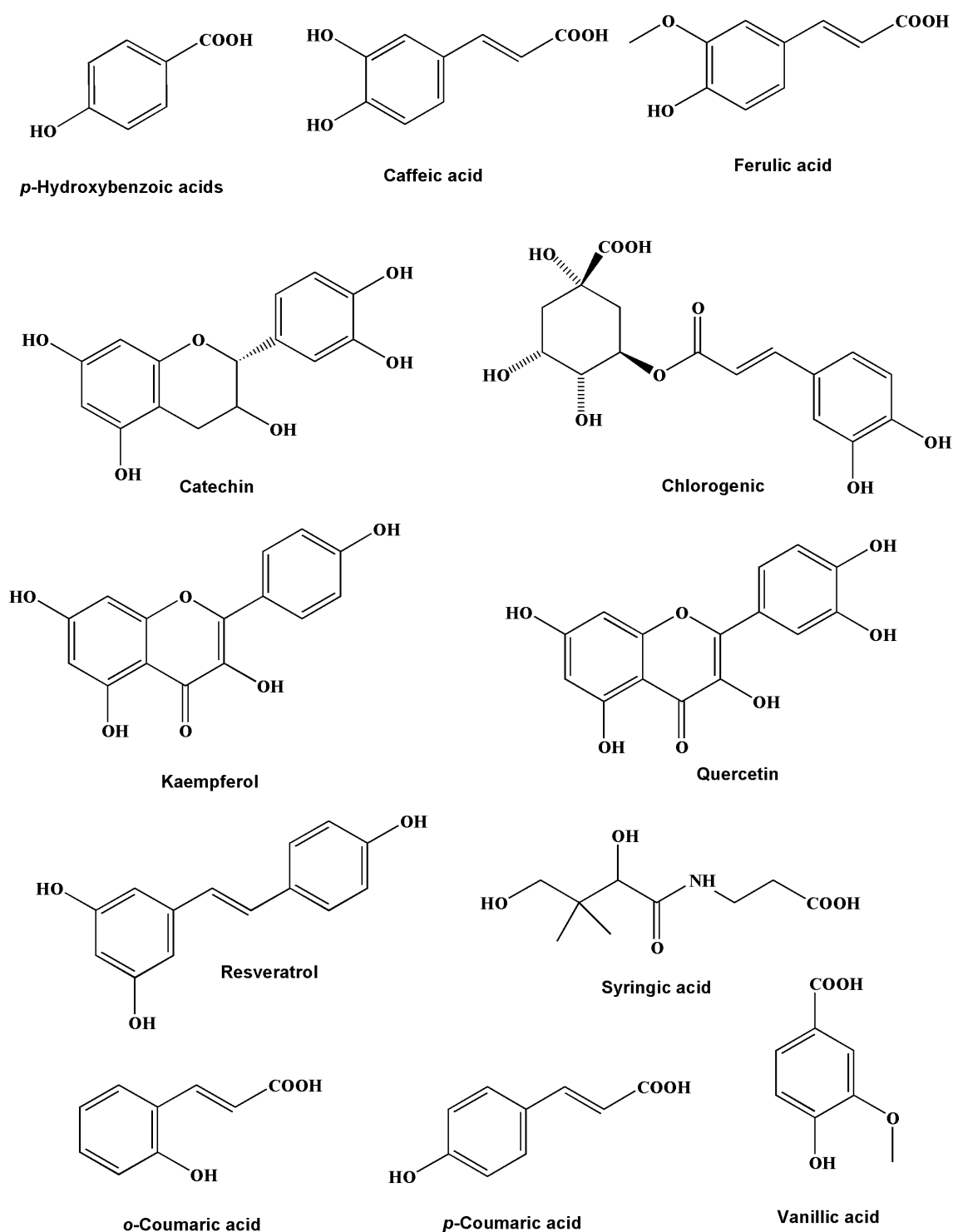
Figure 1. Chemical structures of the polyphenolic compounds in JRPE.

Figure 2C exhibited that the JRPE exerted the maximum ABTS$^{\bullet+}$ scavenging capacity of 98.91% at the highest concentration of 1000 μg/mL, whereas VitC manifested a scavenging capacity of 100% at a concentration of 700 μg/mL. In addition, the IC50 for JRPE was 1202.24 μg/mL, while the IC50 for VitC. was perceived at 345.40 μg/mL.
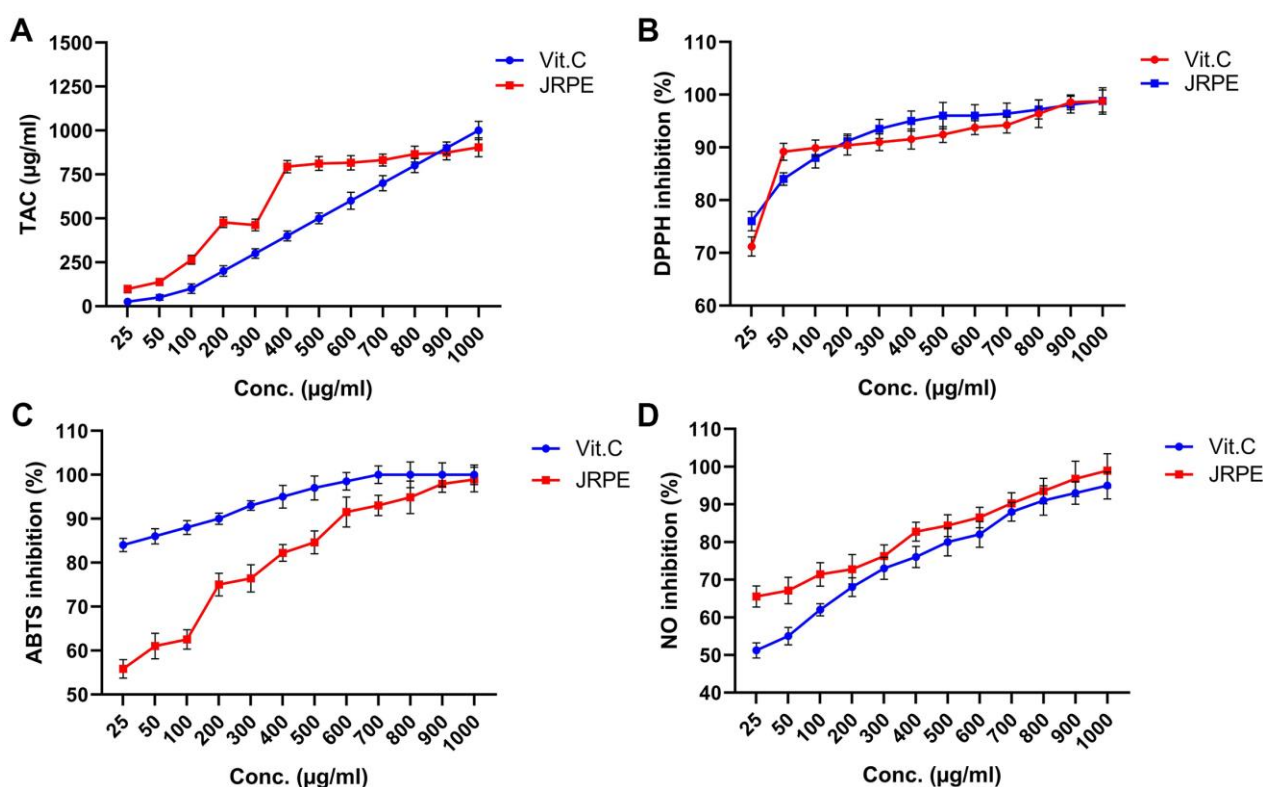
Figure 2. Antioxidant capacity of the JRPE using TAC (**A**), DPPH (**B**), ABTS$^{\bullet+}$ (**C**), and anti-inflammatory using nitric oxide (**D**) compared with VitC as a standard drug. The results are expressed as mean ± SD.

2.3. The Anti-Inflammatory Activity Using Nitric Oxides Assay

The anti-inflammatory activity of the JRPE using the NO model reveals that the JRPE has higher anti-inflammatory activity at all levels compared to VitC with the highest activity of 98.92% at the highest concentration, as portrayed in Figure 2D. Furthermore, the IC50 values for JRPE and VitC in relation to the NO inhibition were reported to be 5326.53 and 5287.20, respectively.

2.4. The Antibacterial Activity of the JRPE

In this work, we also sought to determine whether the JRPE has antibacterial activity against gram-positive (*Streptococcus pyogenes*, *Staphylococcus aureus*, and *Enterococcus faecalis*) and gram-negative (*Escherichia coli* ATCC 8739, *Pseudomonas aeruginosa*, and *Klebsiella pneumonia*). From first sight, it could be discerned that the JRPE exerted significant growth hindrance in relation to the entire indicator bacteria, which was higher than the two reference antibiotics (ampicillin and amoxicillin), and even the later antibiotic is broad-spectrum. The first concentration of the extract (25 µg/mL) revealed low activity against all pathogenic bacteria, which significantly increased with the rise in the concentration of the extract, reaching full bacterial inhibition as presented in Figure 3. The antibacterial findings manifested that the JRPE has remarkable antibacterial properties, particularly against *S. pyogenes* (98.6%) and *S. aureus* (98.69%), which are higher than the antibacterial activities of the empirical antibiotics, ampicillin and amoxicillin. Notably, the JRPE demonstrated almost full bacterial growth inhibition of 99.8% in relation to *Enterococcus faecalis*, whereas ampicillin and amoxicillin exerted growth hindrance ratios of 87.7% and 95.98%, respectively, against the same bacteria. With regard to gram-negative bacteria, the JRPE exhibited a significant growth inhibition of 98.73% toward *E. coli*. By contrast, ampicillin and amoxicillin showed antibacterial rates of 91.68% and 97.05%, respectively, toward

E. coli. In the same manner, the antibacterial capacities of JRPE, ampicillin, and amoxicillin were perceived in relation to *P. aeruginosa* and *K. pneumonia*.
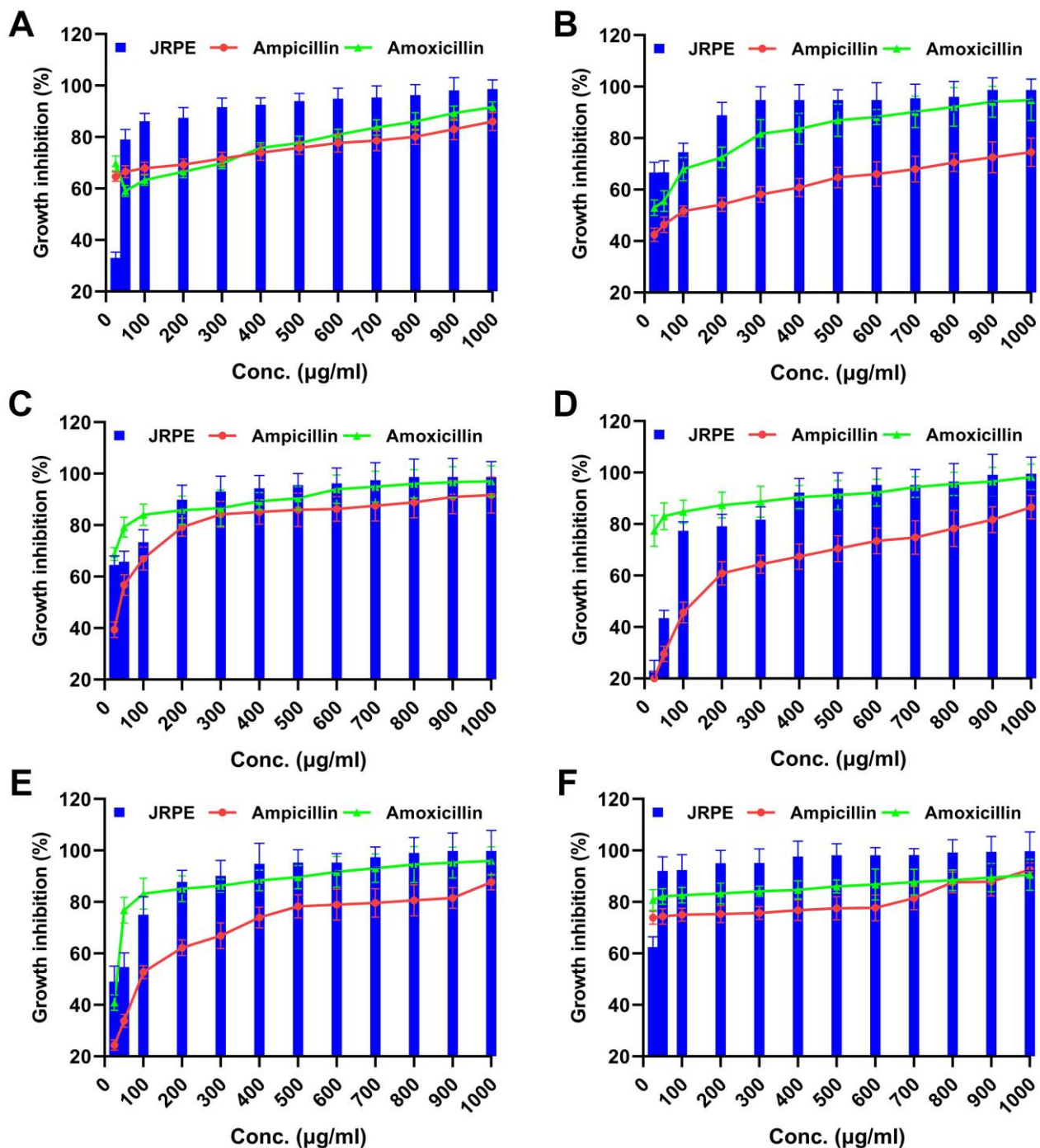

Figure 3. Antibacterial activity of the JRPE compared with two standard antibiotics (ampicillin and amoxicillin) against (**A**) *S. pyogenes*, (**B**) *S. aureus*, (**C**) *E. coli*, (**D**) *P. aeruginosa*, (**E**) *E. faecalis*, and (**F**) *K. pneumonia*. The results are shown as mean ± SD.

2.5. Inhibitory Effects of JRPE toward α-Amylase, Pepsin, Trypsin, and Lipase

The antidiabetic activity of JRPE was evaluated against three digestive enzymes (α-amylase, lipase, and trypsin) as illustrated in Figure 4. Alpha-amylase: considering the α-amylase inhibition after treatment with the JRPE, a minimum enzyme inhibition of 73.71% was detected at a JRPE concentration of 25 µg/mL. Additionally, the enzyme

inhibition was augmented with the increase in JRPE concentration, reporting an inhibitory ratio of 97.43% at 1000 μg/mL. Furthermore, the IC50 value of JRPE against α-amylase was reported to be 2349.16 μg/mL. Lipase: in terms of the lipase enzyme, the minimum inhibition of lipolytic activity was perceived at 25 μg/mL with an inhibition ratio of 38.26%, while the maximum inhibition activity of lipase was 95.96% at 1000 μg/mL with an IC50 of 38.26 μg/mL. Trypsin: the minimum inhibitory activity of trypsin was 30.07% at a concentration of 25 μg/mL. On the other hand, the maximum inhibition of trypsin was 95.48% at 1000 μg/mL with an IC50 value of 517.9548 μg/mL.
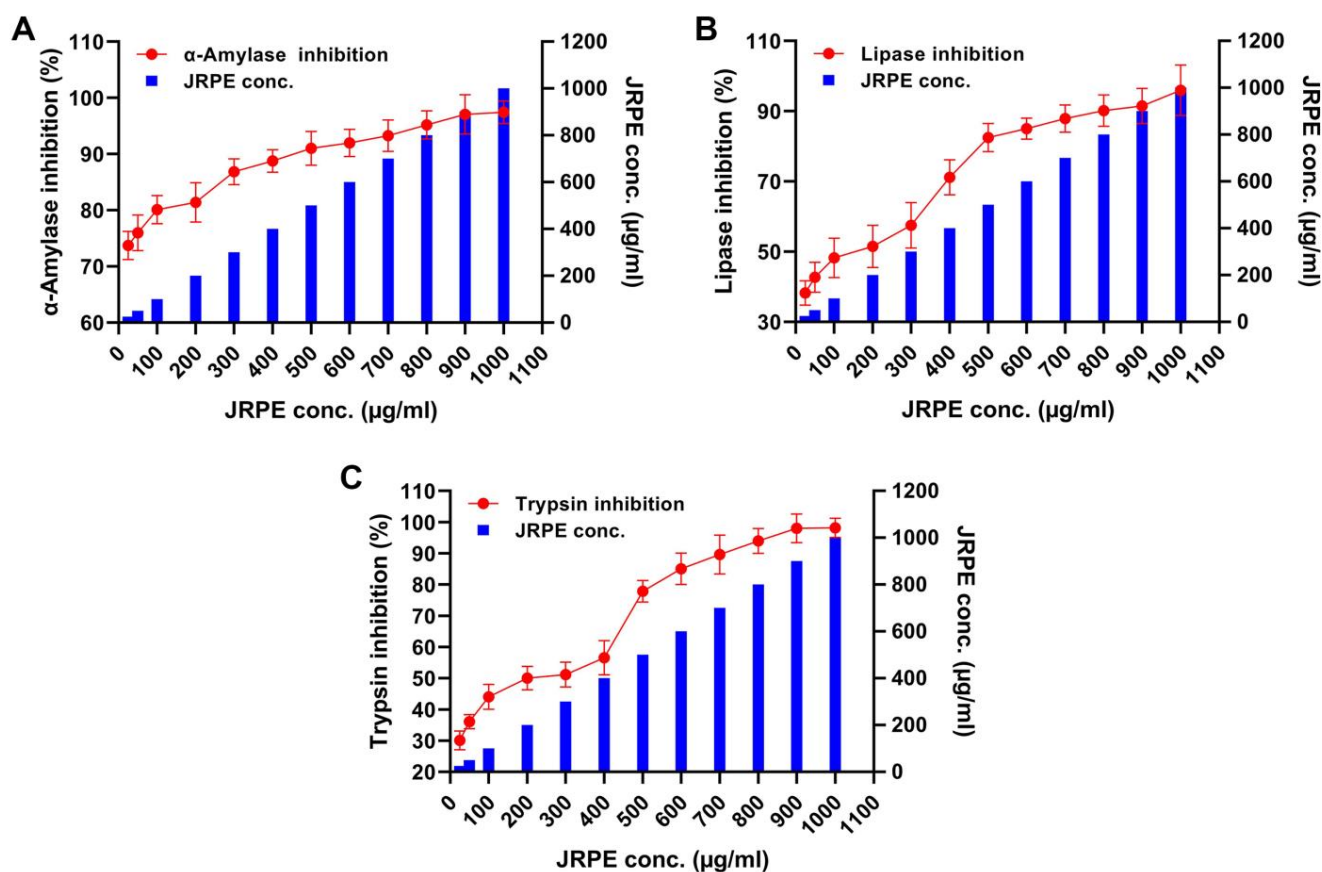

Figure 4. Inhibition properties of JRPE toward (**A**) α-amylase, (**B**) lipase, and (**C**) trypsin. The results are presented as mean ± SD.

2.6. Docking Studies of Polyphenolics in JRPE against Amylase, Lipase, and Trypsin

Docking studies were carried out to assess the interaction and potential binding model, affinity, and binding free energy (ΔG) of the polyphenolics in JRPE in relation to α-amylase, trypsin, and lipase as illustrated in Figures 5–7. The docking scores of the different polyphenolic compounds in the JRPE are enumerated in Table S1. Moreover, the rest of the docking results and the two-dimensional docking analyses for other polyphenolics are illustrated in Tables S2–S4.

Figure 5. The 2D and 3D docking between α-amylase and polyphenolics compound in the JRPE. (**A**) 2D and (**B**) 3D of docking between kaempferol and α-amylase. (**C**) 2D and (**D**) 3D of docking between quercetin and α-amylase. (**E**) 2D and (**F**) 3D of docking analysis between chlorogenic acid and α-amylase.

Figure 6. The 2D and 3D docking between lipase and polyphenolics compound in the JRPE. (**A**) 2D and (**B**) 3D of docking between kaempferol and lipase. (**C**) 2D and (**D**) 3D of docking between quercetin and lipase. (**E**) 2D and (**F**) 3D of docking between chlorogenic acid and lipase.
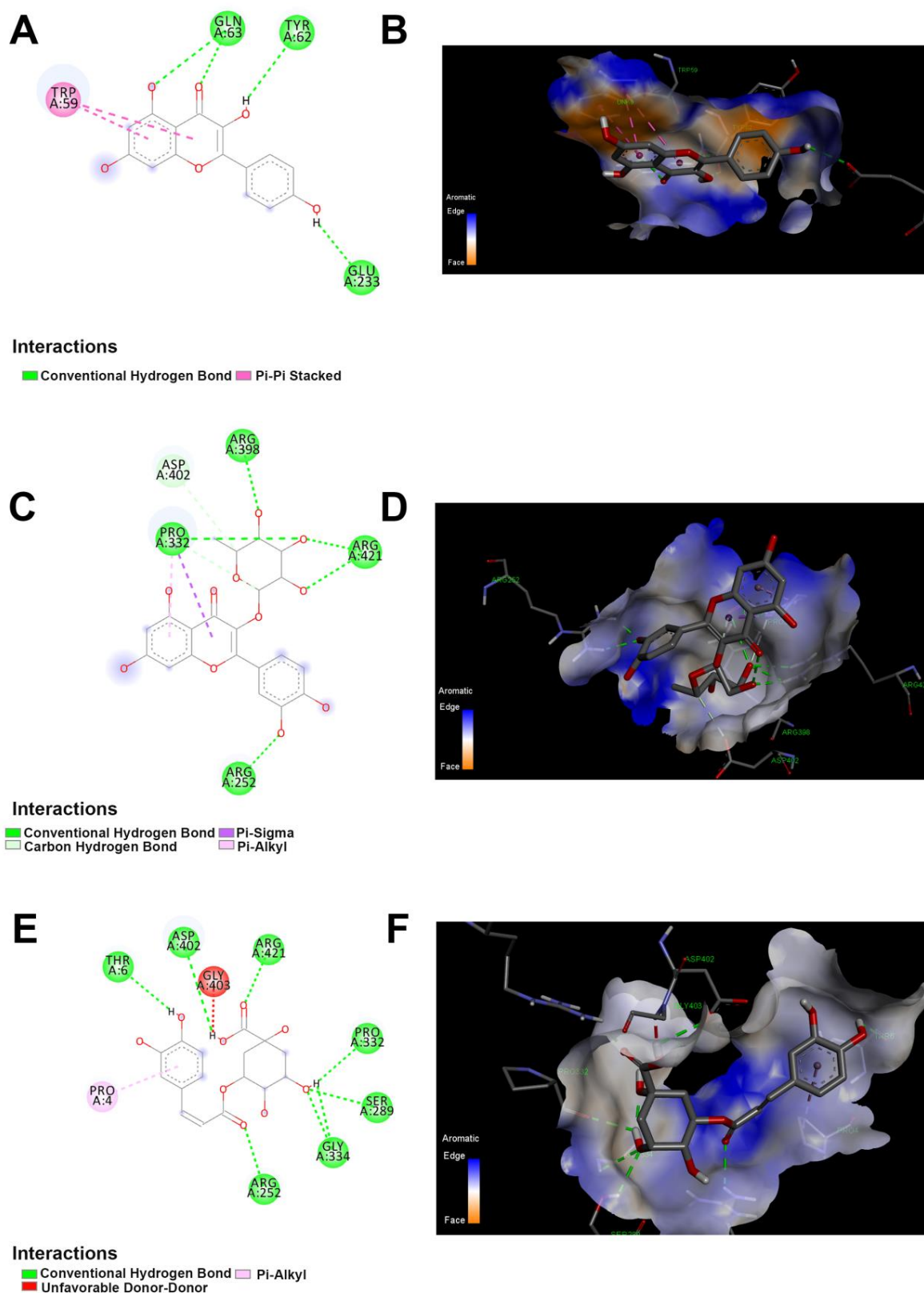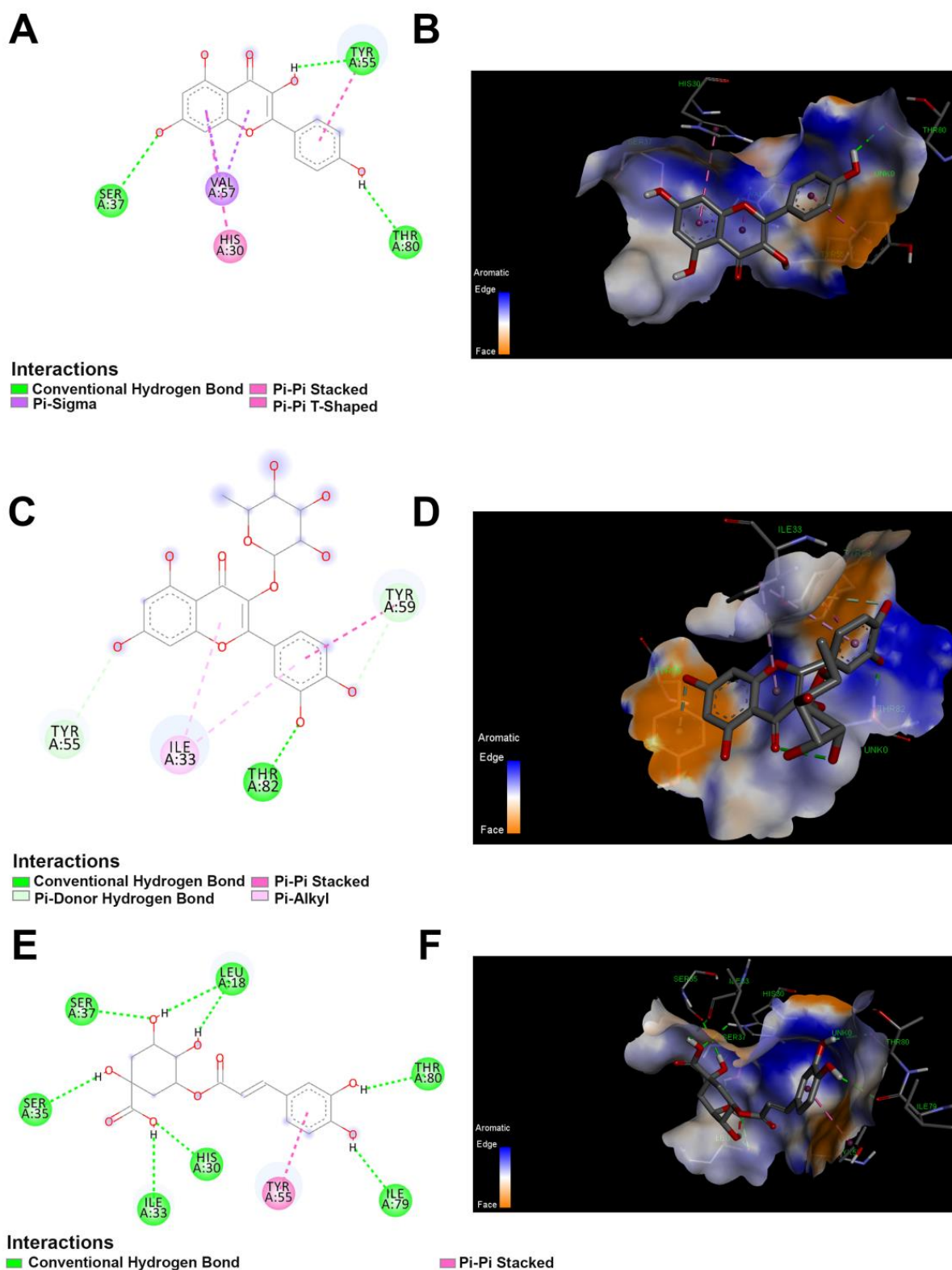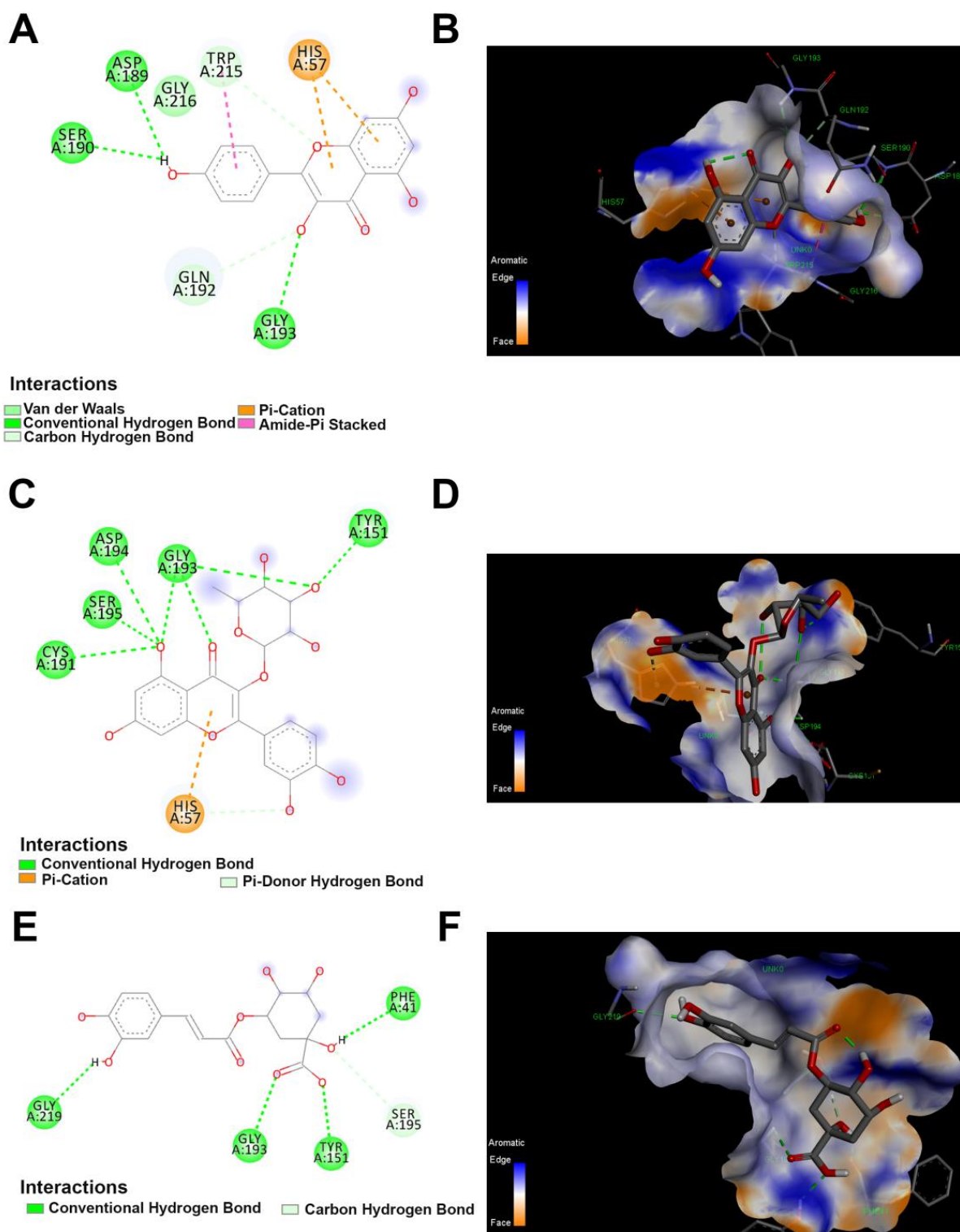
Figure 7. The 2D and 3D docking between trypsin and polyphenolics compound in the JRPE. (**A**) 2D and (**B**) 3D of docking between kaempferol and trypsin. (**C**) 2D and (**D**) 3D of docking between quercetin and trypsin. (**E**) 2D and (**F**) 3D of docking between chlorogenic acid and trypsin.

2.7. Interactions Assessment between the Twelve Polyphenolic Compounds and α-Amylase

According to the results obtained from in vitro studies, the computational docking analyses indicated that the twelve compounds could bind to the active site of α-amylase with the lowest binding energies of −4.5, −5.3, −6.43, and −5.7 kcal/mol, respectively,

as presented in Table S1. Among all compounds, kaempferol, quercetin, and chlorogenic acid exhibited the highest docking scores of −8.4, −8.8, and −8 kcal/mol, respectively. As shown in Figure 5, all these residues are involved in the enzyme's binding to the docked compounds. Noticeably, the quercetin demonstrated the highest affinity score of −8.8 with α-amylase, revealing the interaction between the α-amylase and quercetin as shown in Figure 6. Furthermore, the amino acid residues (ARG A:398, PRO A:332, ARG A:421, and ARG A:252) exhibited a standard hydrogen bond with α-amylase. In addition, the ASP A:402 showed a carbon-hydrogen bond, whereas the PRO A:332 revealed p-alkyl and p-sigma bonds. The interaction of kaempferol with α-amylase exposed the second highest affinity score of −8.4, showing two types of interaction bond, including the conventional hydrogen bond (GLN A:63, TYR A:62, GLU A:233), and Pi–Pi stacked (TRP A:59). Chlorogenic acid demonstrated the third highest affinity score of −8, showing two types of interaction bonds, involving conventional hydrogen bonds (THR A:6, ASP A:402, ARG A:421, PRO A:332, SER A:289, GLY A334, ARG:252) and pi–Alkyl bonds (PRO A:4).

2.8. Interactions between the Twelve Polyphenolic Compounds and Lipase

Based on the findings of the in vitro investigations, the computational docking results exhibited that the twelve compounds attached to the active site of the lipase enzyme were catechin, *p*-coumaric acid, and vanillic acid with the lowest binding energies of −4.1, −4.3, and −4.3, kcal/mol, respectively. Out of the entire compounds, kaempferol, quercetin, and chlorogenic acid demonstrated the highest docking scores of −7.1, −7.4, and −7.2 kcal/mol, respectively. All these residues that participated in the enzyme binding to the docked compounds are represented in Table S1. The interaction between quercetin and lipase showed four types of interaction bonds, including the standard hydrogen bond (THR A:82), the pi–donor hydrogen bond (TYR A:59), (Pi–Pi stacked TYR A:59), and (Pi–Alkyl ILE A:33) as delineated in Figure 6. For kaempferol interaction bonds, it showed also four types of interaction bond, involving conventional (SER A:37, TYR A:55, THR A:80), pi–sigma (VALA: 57), Pi–Pi stacked (His A:30), and Pi–Pi shaped (TYR A:55). On the other hand, the chlorogenic acid had two types of interaction bonds: (SER A:37, SER A:35, LEU A:18, ILEA:33, HIS A:30, THR A:80, ILE A:79), and Pi–stacked (TYR A:55).

2.9. Interactions between the Twelve Polyphenolic Compounds and Trypsin

The computational docking results indicated that the twelve compounds bound to the active site of trypsin with the lowest binding energies of −4.1, −4.3, and −4.3, kcal/mol, for catechin, *p*-coumaric acid, and vanillic acid, respectively. As mentioned above in the docking analysis for lipase, the highest docking scores were observed for kaempferol, quercetin, and chlorogenic acid with affinity scores of −7.2, −7.2, and −7.1 kcal/mol, respectively. All these residues are contributed in the enzyme binding and the docked compounds are illustrated in Table S1. The interaction between lipase and quercetin is shown in Figure 7. Specifically, the interaction between quercetin and trypsin showed four types of interaction bonds, involving the conventional hydrogen bond (THR A:82), the pi–donor hydrogen bond (TYR A:59), Pi–Pi stacked (TYR A:59), and the pi–Alkyl bond (ILE A:33). Similarly, kaempferol docking with trypsin revealed conventional (SER A:37, TYR A:55, THR A:80), pi–sigma (VALA: 57), pi–pi stacked (His A:30), and pi–pi shaped (TYR A:55) interaction bonds. As observed above in the docking of lipase, chlorogenic acid displayed two types of interaction bonds: (SER A:37, SER A:35, LEU A:18, ILEA:33, HIS A:30, THR A:80, ILE A:79), and Pi–stacked (TYR A:55).

2.10. Pharmacodynamics and Pharmacokinetics of Polyphenolics Composition in JRPE

The pharmacokinetics, medicinal chemistry, drug-likeness, physicochemical properties, lipophilicity, and water solubility data are summarized in Table S5. According to the pharmacokinetic and ADMET properties, JRPE showed a high human intestinal absorption rate for almost all compounds, with the exception of chlorogenic acid and quercetin, which revealed a low intestinal absorption rate. Furthermore, polyphenolic compounds in the

JRPE exposed very low BBB permeability except for five compounds, involving *o*-coumaric, *p*-coumaric, ferulate, *p*-hydroxybenzoic acid and resveratrol. On the other hand, JRPE showed no effect on cytochrome P450 isomers for eight compounds, including caffeic, ferulate, quercetin, 4-hydroxybenzoic acid, chlorogenic acid, *p*-coumaric acid, *o*-coumaric acid, syringic acid, and vanillic acid. Most importantly, JRPE toxicity (non-mutagenic), hepatotoxicity, or skin sensitization were not perceived in the JRPE.

3. Discussion

In this study, the influence of *Jania rubens* polyphenolic extract (JRPE) on the activity of three common digestive enzymes, including α-amylase, lipase, and trypsin was investigated to comprehend their potential application as anti-obesity and anti-diabetic extract. Moreover, the antibacterial, anti-inflammatory, and antioxidant properties of JRPE polyphenols were examined. The polyphenolic contents bestow on JRPE the competency to deactivate various digestive enzymes. Thus, we investigated the inhibition of α-amylase, lipase, and trypsin activities by JRPE. After treatment with JRPE, the maximum inhibition ratios of -amylase, trypsin, and lipase were reported to be 97.43%, 98.20%, and 95.96%, respectively. This implies that the JRPE may have powerful anti-diabetic and anti-obesity properties. It is believed that polyphenol chemicals possess substantial antioxidant and antibacterial properties. Nevertheless, due to the binding of polyphenols and proteins, they are impounded into either soluble or insoluble complexes, which may frustrate the function of both polyphenols and proteins [11,24]. This makes seaweed extracts a promising candidate for the expansion of natural alternatives to synthetic compounds applied in food and cosmetic production [25–29].

The attachment of polyphenols to proteins can alter the structure, solubility, hydrophobicity, thermal stability, and isoelectric point of the protein by blocking specific amino acids, which certainly instigates conformational remodeling of the protein. Given the protein-phenolic complex, the digestibility and exploitation of dietary proteins, in addition to the activity of digestive enzymes, are altered [30,31]. Naturally occurring polyphenols have been shown to inhibit the activity of various digestive enzymes, including α-glycosidase, α-amylase, lipase, and trypsin [32]. This alters the nutrient availability and, in turn, the microbiota composition.

Considering the antibacterial activity of polyphenols, they have been evinced to have antibacterial effects by binding and inactivating essential bacterial proteins such as adhesins, enzymes, and cell envelope transport proteins. Previous studies reported that kaempferol and its derivatives could thwart the replication of *Streptococcus mutans* through disruption of a membrane enzyme identified as sortase A. Since this enzyme is vitally responsible for bacterial adherence and host cell invasion, it significantly contributes to the pathogenicity and even the virulence of the bacteria [33]. Moreover, recent studies evidenced the potent inhibitory impacts of quercetin, flavonoids, rutin, and phenolic acid against sortases A and B of *S. aureus* [34,35]. Inhibition of bacterial nucleic acid production is likely related to the B ring of the flavonoids intercalating or forming a hydrogen bond with the stacking of nucleic acid bases. Lou et al. [36] postulated two mechanisms to decipher the bactericidal activity of *p*-coumaric acid: (I) binding to bacterial genomic DNA, resulting in suppression of various metabolic pathways and, ultimately, cell death; and (II) disruption of bacterial cell membranes. It is worth mentioning that previous investigations highlighted the competency of chlorogenic acid to thwart biofilm production, swarming, and other virulence influences such as protease and elastase activity in *P. aeruginosa* along with the disordering of other mechanisms such as rhamnolipid and pyocyanin synthesis [37,38]. Likewise, quercetin effectively inhibited biofilm formation in *K. pneumoniae*, *P. aeruginosa*, and *Y. enterocolitica*, as well as other quorum-sensing-regulated attributes; for instance, inhibition of violacein and production of exopolysaccharide production as alginate [35]. Crucially, the swimming and swarming of *P. aeruginosa* and *Y. enterocolitica* were also drastically suppressed by quercetin [39,40]. Besides, resveratrol as another phenolic compound, it has the competency to disturb the physicochemical properties of the surface of *Lactobacillus paracasei*. More-

over, the adhesion, bacterial aggregation, and biofilm capabilities were also blocked as a consequence of *L. paracasei* treatment with resveratrol [41]. Overall, the substantial antibacterial activity of the JRPE compared to a broad-spectrum antibiotic, such as amoxicillin is most likely due to the synergistic influence of the polyphenolic compounds implicated in the extract.

In addition, we also studied the inhibitory impacts of the twelve polyphenolic compounds against digestive enzymes. The synergistic/antagonistic actions among bioactive features in JRPE may account for why it has a greater pancreatic digestive-inhibitory effect than other extracts with similar activity levels [42]. The systems were characterized by a predominance of the competitive part of mixed inhibition. These findings support the hypothesis that polyphenolic extract inhibits the activity of pancreatic α-amylase, lipase and trypsin through competitive mechanisms [43]. Additionally, the effect of quercetin on other pancreatic enzymes, including α-amylase, was previously investigated [44].

To determine the potential binding sites of polyphenolics with pancreatic enzymes (α-amylase, lipase, and trypsin), docking analyses were conducted employing the structures of all compounds. The competitive component of the polyphenolic compounds' mixed-inhibition may be explained by their interactions with residues close to the active site. Taking into account that the enzyme inhibitors interact with the substrate–enzyme, binding may shed light on the inhibitory process. To reiterate, the inhibitor would bind not to the substrate–enzyme combination itself but to the enzyme itself, and it would do so in close proximity to the substrate binding site.

The binding to the active site attains in a fashion that only influences on the catalytic cascades and not the substrate binding, which may explain why polyphenolic compound mixed-type inhibition is non-competitive. Zhu et al. [45] reported that polyphenolic substances could bind to a pancreatic lipase through hydrophobic interactions. For instance, pancreatic digesting enzymes and aromatic rings from polyphenolic substances generate π-stacking interactions. Our findings are in line with those of Swilam et al. [46], who observed that hydrophobic bonds were the primary form of interaction between polyphenolic chemicals and digestive enzymes. Furthermore, it was predicted by the docking study that the hydroxyl groups of polyphenolics and the polar groups of digestive enzymes could form a hydrophobic bond [47]. Compared to other polyphenolic compound–pancreatic lipase complexes, the quercetin–digestive enzyme complex had greater polar interactions. The larger size and rigid structure of quercetin may account for its predominant binding qualities (more polar contacts) and, by extension, its greater inhibitory competency in the digestive tract. Zhang et al. [48] also found that quercetin was more effective at inhibiting the target enzyme. Moreover, Ullah et al. [49] demonstrated that quercetin has a stronger affinity for proteins due to its structural features. The catechol structure in the B ring and the double bond between C2 and C3 are two of quercetin's distinguishing features. The capability of polyphenolics to bind proteins is predominantly correlated to structural features, including free hydroxyl groups and number of aromatic rings and [50].

4. Materials and Methods

4.1. Samples Collection

Jania rubens was collected during 2019 at a depth of 1–27 m in the Red Sea region, Hurghada (latitude: 27°11′37.5″ and longitude: 33°50′48.4″), Egypt and immediately transported to the lab. The collected samples were identified at the National Institute of Oceanography and Fisheries (NIOF), Egypt.

4.2. Extraction and Preparation of Jania rubens Polyphenolic Extract (JRPE)

To extract the polyphenolic compounds from *Jania rubens*, the samples were dried in air before being ground to obtain the powder with a weight of 500 g. Afterward, the powder was immersed in ethyl acetate for 1 h, followed by sonication before being maintained overnight in the fridge at 4 °C in the dark bottle. The extraction process was conducted three times to maximize the yield of polyphenolic compounds. Following this,

the solvent was eliminated by means of a rotary evaporator (R-300, Büchi Labortechnik GmbH, Essen, Germany) at 45 °C under a low pressure before being stored at 4 °C for further investigations [49,50].

4.3. High-Performance Liquid Chromatography (HPLC) Analysis of JRPE

To ascertain the phenolic and flavonoid compounds in the JRPE, HPLC analysis was performed by means of HPLC (Agilent 1260, Santa Clara, CA, USA) using a Kinetex® 5 μm EVO C18 column (100 mm × 4.6 mm) purchased from Phenomenex®, Torrance, CA, USA. The separation was accomplished utilizing a tertiary liner elution gradient with HPLC grade water, 0.2% H_3PO_4 (*v/v*), methanol, and acetonitrile. The injection volume was 20 μL, and the detection was performed using WWD at 284 nm.

4.4. Antioxidant Activity of JRPE

To assess the antioxidant properties of the JRPE, DPPH and ABTS$^{\bullet+}$ assays were conducted using 2,2-diphenyl-1-picrylhydrazyl and 2,2′-azino-bis(3-ethylbenzothiazoline-6-sulfonic acid), respectively, following the previous protocols with minor adaptations [51,52]. All investigations were performed in triplicate, and the free radical scavenging was then calculated using Equation (1):

$$\text{Scavenging (\%)} = [(A_c - A_s)/A_c] \times 100 \tag{1}$$

where Ac and As point to the absorbance of the control and the sample after reaction, respectively.

To assess the total antioxidant capacity (TAC) of the JRPE, the phosphomolybdenum approach was performed following the procedures reported by Prieto et al. [53]. Vitamin C (VitC) was utilized as a standard, and the reactions were replicated three times.

4.5. Anti-Inflammatory Activity of JRPE

To estimate the anti-inflammatory properties of the JRPE, a nitric oxide scavenging approach was performed in accordance with the protocol delineated by Garrat [54]. Vit. C was applied as a standard drug in this assay, and the investigations were accomplished in triplicate. The inhibition ratio of nitric oxide was computed using Equation (2):

$$\text{Nitric oxide scavenging (\%)} = [(A_c - A_s)/A_c] \times 100. \tag{2}$$

where Ac is the absorbance of the control, while as indicates the absorbance of the sample after reaction.

4.6. Antibacterial Assessments of JRPE

The antibacterial properties of JRPE were evaluated toward three gram-positive bacteria (*Streptococcus pyogenes* ATCC 19615, *Staphylococcus aureus* ATCC 25923, *and Enterococcus faecalis* ATCC 29212) and three gram-negative bacteria (*Escherichia coli* ATCC 8739, *Pseudomonas aeruginosa* ATCC 15442, and *Klebsiella pneumoniae* ATCC 13883) in accordance with the resazurin assay using a microtiter plate (Sigma-Aldrich, Taufkirchen, Germany). Each bacterial strain was revitalized by growing overnight at 37 °C in LB medium, followed by adjustment of their turbidities at 600 nm by means of a spectrophotometer in compliance with the McFarland 0.5 standard [55,56]. A volume of 50 μL representing different concentrations of the JRPE from 25 to 1000 μg/mL) was loaded into a sterile microtiter plate (96-well), followed by the addition of 10 μL of resazurin indicator solution to each well. Following this, 30 μL of LB medium was added to the wells before being inoculated with 10 μL of bacterial suspension (5×10^6 CFU/mL). Ampicillin and amoxicillin (Sigma-Aldrich, Taufkirchen, Germany) were applied as reference antibiotics to the microtiter plate with concentrations comparable to the extract. To avoid the rehydration of bacteria, each plate was wrapped with cling film before being incubated overnight at 37 °C. The antibacterial evaluations were carried out in triplicate and the bacterial cultures in each microplate were

measured at 520 nm by means of a microplate reader (SpectraMax i3x Multi-Mode, San Jose, CA, USA). The growth inhibition ratio of bacteria was quantified using Equation (3):

$$\text{Growth inhibition of bacteria (\%)} = [(Ac - As)/Ac)] \times 100 \tag{3}$$

where Ac and As indicate the absorbance of untreated bacterial cultures and bacterial cultures treated with JRPE, respectively.

4.7. Anti-Diabetics and Anti-Obesity of JRPE Using Inhibition of Digestive Enzymes

The anti-diabetics and anti-obesity of JRPE were evaluated utilizing α-amylase, lipase, and trypsin (Loba chemie, Mumbai, India). To estimate the activity of pancreatic α-amylase activity, we utilized soluble starch as a substrate and the reducing sugars were then calorimetrically evaluated adopting the dinitrosalicylic acid method demonstrated by Miller [57]. The reaction was performed by adding 20 μL of α-amylase solution containing 20 μg of the enzyme to 280 μL of starch solution (1%, *w/v*) prepared in phosphate buffer (pH 7) supplemented with 20 mM $CaCl_2$. The reaction was commenced by incubation at 37 °C before being terminated by the addition of a DNSA reagent. To evaluate the ability of the JRPE to inhibit the α-amylase activity, different concentrations of the extract from 25 to 1000 μg/mL were added to 20 μL of α-amylase enzyme solutions before being incubated for 5 min. Following this, the enzyme activity was estimated using the DNS method and measured at 540 nm by means of a spectrophotometer.

To assess the lipase inhibition, a stock solution of pancreatic lipase (1 mg/mL) was prepared in 10 mM Tris-HCl buffer (PH 7.5). The lipase activity was assayed as previously described by Choi et al. [58] with slight modifications. DMPTB (2,3- mercapto-1-propanol tributyrate) was utilized as a substrate and dissolved in 50 mM Tris-HCl buffer (PH 7.2) complemented with 6% of Triton X-100, while the DTNB reagent (5,5-dithio-bis-(2-nitrobenzoic acid) at concentration of 40 mM was prepared in isobutanol. The lipase inhibition using the JRPE was conducted using different concentrations within a range from 25 to 1000 μg/mL. The reaction was performed by adding 200 μL from each concentration of JRPE to 100 μL of the enzyme solution, followed by addition of 700 μL of tris-HCl buffer (pH 7.4) to the mixture. After incubation of the tubes at 37 °C for 15 min, 100 μL of DMPTB substrate was added to the mixture for the enzyme assay. The activity of the lipase enzyme was evaluated at 405 nm employing a spectrophotometer.

For estimating the capacity of the JRPE to inhibit the activity of trypsin, 1.5 mL of trypsin solution prepared in Tris-HCl buffer (0.2 M, pH 8) was pre-incubated at 25 °C for 15 min with 1.5 mL of different concentrations of JRPE, ranging from 25 to 1000 μg/mL. Casein was used as a substrate and was prepared in Tris-HCl buffer (0.2 M, pH 8) supplemented with 20 mM $CaCl_2$ in a ratio of 1:1.8, respectively, before being incubated in a water bath at 37 °C for 20 min to fully dissolve. To estimate the enzyme activity, 2.8 mL of the substrate was thoroughly mixed with 200 μL of the enzyme and JRPE. After incubation for 20 min at 37 °C, the reaction was terminated by adding 6 mL of 2.5% trichloroacetic acid (TCA) and the tubes were then maintained on ice for 20 min. The tubes were centrifuged at 10,000 rpm for 10 min, and the supernatants were further measured at 280 nm using a spectrophotometer. The inhibition percentage was calculated using Equation (4):

$$\text{Enzyme inhibition (\%)} = [(Ac - At)/Ac] \times 100 \tag{4}$$

where Ac points to the absorbance of the control, which contains all reagents and 20% DMSO in the absence of the tested solution, while At indicates the absorbance of the examined sample.

The half-maximal inhibitory concentration (IC50) values were estimated following fitting inhibition parameters with standard log inhibitor vs. normalized response models using AAT Bioquest (https://www.aatbio.com/tools/ic50-calculator, accessed on 20 November 2022).

4.8. Molecular Docking Studies

The crystal structures of α-amylase (PDB ID: 4W93), lipase (PDB ID: 1LPB), and trypsin (PDB ID: 4DOQ) were retrieved from the Protein Data Bank website: http://www.rcsb.org (accessed on 20 November 2022) and the target proteins were prepared for docking analysis employing Pymol Opensource, Shirley, NY, USA. Furthermore, to prepare the ligands, the 3D structures of the investigated 12 polyphenolic compounds and the co-crystallized compound were obtained from the PubChem database (www.pubchem.ncbi.nlm.nih.gov (accessed on 20 November 2022)) and their chemical structures were then transformed into PDB using Pymol [59]. Afterward, the ligands were transformed into PDBQT format by means of AutoDock Tools, San Diego, CA, USA for molecular docking simulation. Before commencing the docking examinations, the docking procedure was verified by redocking the native inhibitors into the active site of the enzyme. The binding model with the minimum binding energy was superimposed on the retrieved co-crystallized inhibitor. Then, polyphenolics in JRPE were docked into the active sites of the enzymes employing the AutoDock Vina docking system. The prepared structures of enzymes were also imported, and the docking examination was commenced with all other parameters. The docked complexes were visualized by means of the Discovery Studio Visualizer, Shirley, NY, USA (V. 21) to explore and report the different molecular interactions.

4.9. In Silico Pharmacodynamics and Pharmacokinetics

To assess the drug-likeness of the 12 polyphenolic compounds in JRPE, in silico evaluation was attained adopting (http://www.swissadme.ch/index.php#, accessed on 20 November 2022) [60] based on specific properties of compounds, including absorption, distribution, metabolism, and excretion as assessments for pharmacokinetic features [61].

4.10. Statistical Analysis

All the experimental assays were carried out at least in triplicate, and results are shown as mean $\pm$ SD. The results were analyzed by means of GraphPad Prism (Version 8, GraphPad Software Inc., San Diego, CA, USA) and were considered to be significant at $p \leq 0.05$.

5. Conclusions

Twelve polyphenolic compounds were identified in the extract of *Jania rubens* (JRPE) collected from Egypt. The JRPE demonstrated remarkable antioxidant and antibacterial activities. Among the identified polyphenolic compounds, quercetin, kaempferol, and chlorogenic exposed the highest inhibition toward α-amylase, lipase, and trypsin with acceptable IC$_{50}$. This may be related to the antioxidant and anti-inflammatory properties of JRPE extract, which enable them to bind with digestive enzymes, forming a polyphenolic-enzyme complex. Furthermore, computational studies following molecular docking analysis for the twelve polyphenolic compounds in JRPE exhibited that the polyphenolics may develop a complex with digestive enzymes, demonstrating that all compounds could closely bind to the active site of digestive enzymes. Significantly, the in vitro studies substantiated the powerful inhibitory activity of JRPE, indicating the anti-obesity and anti-diabetes characteristics of the implicated polyphenolic compounds. Further in vivo investigations should be performed to evaluate the capacity of the JRPE to govern diabetes in animal models, and the polyphenolic compounds could be purified to assess their independent bioactivity.

Supplementary Materials: The following supporting information can be downloaded at: https://www.mdpi.com/article/10.3390/catal13020443/s1, Figure S1: HPLC chromatogram for the JRPE shows different polyphenolic compounds (phenolic and flavonoids); Table S1: The docking affinity scores of the different polyphenolics' compounds in the JRPE; Table S2: Affinity scores for docking analysis of α-amylase (PDB ID: 4W93) using twelve polyphenolic compounds identified from JRPE; Table S3: Affinity scores for docking analysis of lipase (PDB ID: 1LPB) using twelve polyphenolic compounds identified from JRPE; Table S4: Affinity scores for docking analysis of trypsin (PDB ID:

4DOQ) using twelve polyphenolic compounds identified from JRPE; Table S5: Pharmacodynamics and pharmacokinetics analysis of twelve polyphenolic compounds identified from JRPE.

Author Contributions: Conceptualization, A.N.-A., M.A.S. and M.A.H.; data curation, A.N.-A. and M.A.H.; investigation, A.N.-A. and M.A.H.; formal analysis, A.N.-A., M.L.A., T.M.T. and M.A.H.; writing—original draft, A.N.-A. and M.A.H.; writing—review and editing, A.N.-A., M.L.A., T.M.T., M.A.S. and M.A.H. All authors have read and agreed to the published version of the manuscript.

Data Availability Statement: The datasets generated during the current study are available from the corresponding authors upon reasonable request.

Conflicts of Interest: The authors declare no conflict of interest.

References

1. Forouhi, N.G.; Wareham, N.J. Epidemiology of diabetes. *Medicine* **2014**, *42*, 698–702. [CrossRef]
2. Federation, I.D. *IDF Diabetes Atlas*, 9th ed.; International Diabetes Federation: Brussels, Belgium, 2019; Available online: https://www.diabetesatlas.org (accessed on 20 November 2022).
3. Galicia-Garcia, U.; Benito-Vicente, A.; Jebari, S.; Larrea-Sebal, A.; Siddiqi, H.; Uribe, K.B.; Ostolaza, H.; Martín, C. Pathophysiology of Type 2 Diabetes Mellitus. *Int. J. Mol. Sci.* **2020**, *21*, 6275. [CrossRef] [PubMed]
4. Rajasekaran, P.; Ande, C.; Vankar, Y.D. Synthesis of (5,6 & 6,6)-oxa-oxa annulated sugars as glycosidase inhibitors from 2-formyl galactal using iodocyclization as a key step. *ARKIVOC* **2022**, *2022*, 5–23.
5. Yang, L.-F.; Shimadate, Y.; Kato, A.; Li, Y.-X.; Jia, Y.-M.; Fleet, G.W.J.; Yu, C.-Y. Synthesis and glycosidase inhibition of N-substituted derivatives of 1,4-dideoxy-1,4-imino-d-mannitol (DIM). *Org. Biomol. Chem.* **2020**, *18*, 999–1011. [CrossRef] [PubMed]
6. Anand, U.; Jacobo-Herrera, N.; Altemimi, A.; Lakhssassi, N. A Comprehensive Review on Medicinal Plants as Antimicrobial Therapeutics: Potential Avenues of Biocompatible Drug Discovery. *Metabolites* **2019**, *9*, 258. [CrossRef] [PubMed]
7. Shreadah, M.A.; El Moneam, N.; El-Assar, S.A.; Nabil-Adam, A. Metabolomics and pharmacological screening of aspergillus versicolor isolated from *Hyrtios erectus* Red Sea sponge; Egypt. *Curr. Bioact. Compd.* **2020**, *16*, 1083–1102. [CrossRef]
8. Nabil-Adam, A.; Shreadah, A.M.; Abd El-Moneam, M.N.; El-Assar, A.S. Marine Algae of the Genus Gracilaria as Multi Products Source for Different Biotechnological and Medical Applications. *Recent Pat. Biotechnol.* **2020**, *14*, 203–228. [CrossRef] [PubMed]
9. AbdelMonein, N.M.; Yacout, G.A.; Aboul-Ela, H.M.; Shreadah, M.A. Hepatoprotective Activity of Chitosan Nanocarriers Loaded with the Ethyl Acetate Extract of a *Stenotrophomonas* sp. Bacteria Associated with the Red Sea Sponge Amphimedon ochracea in CCl4 Induced Hepatotoxicty in Rats. *Adv. Biosci. Biotechnol.* **2017**, *8*, 27–50. [CrossRef]
10. Abd El-Moneam, N.M.; Shreadah, M.A.; El-Assar, S.A.; Nabil-Adam, A. Protective role of antioxidants capacity of *Hyrtios aff. Erectus* sponge extract against mixture of persistent organic pollutants (POPs)-induced hepatic toxicity in mice liver: Biomarkers and ultrastructural study. *Environ. Sci. Pollut. Res.* **2017**, *24*, 22061–22072. [CrossRef]
11. Abd El-Moneam, N.M.; El-Assar, S.A.; Shreadah, M.A.; Nabil-Adam, A. Isolation, identification and molecular screening of Pseudomonas sp. metabolic pathways NRPs and PKS associated with the Red Sea sponge, *Hyrtios aff. Erectus*, Egypt. *J. Pure Appl. Microbiol.* **2017**, *11*, 1299–1311. [CrossRef]
12. Wang, C.C.L.; Hess, C.N.; Hiatt, W.R.; Goldfine, A.B. Clinical Update: Cardiovascular Disease in Diabetes Mellitus. *Circulation* **2016**, *133*, 2459–2502. [CrossRef]
13. Chaudhury, A.; Duvoor, C.; Reddy Dendi, V.S.; Kraleti, S.; Chada, A.; Ravilla, R.; Marco, A.; Shekhawat, N.S.; Montales, M.T.; Kuriakose, K.; et al. Clinical Review of Antidiabetic Drugs: Implications for Type 2 Diabetes Mellitus Management. *Front. Endocrinol.* **2017**, *8*, 6. [CrossRef] [PubMed]
14. Janssen, J.A.M.J.L. Hyperinsulinemia and Its Pivotal Role in Aging, Obesity, Type 2 Diabetes, Cardiovascular Disease and Cancer. *Int. J. Mol. Sci.* **2021**, *22*, 7797. [CrossRef]
15. Gong, L.; Feng, D.; Wang, T.; Ren, Y.; Liu, Y.; Wang, J. Inhibitors of α-amylase and α-glucosidase: Potential linkage for whole cereal foods on prevention of hyperglycemia. *Food Sci. Nutr.* **2020**, *8*, 6320–6337. [CrossRef] [PubMed]
16. Arbi, B.; Bouchentouf, S.; El-Shazly, M. Investigation Of The Potential Antidiabetic Effect Of *Zygophyllum* Sp. By Studying The Interaction Of Its Chemical Compounds With Alpha-Amylase And Dpp-4 Enzymes Using A Molecular Docking Approach. *Curr. Enzym. Inhib.* **2023**, *19*. [CrossRef]
17. Abol-Fotouh, D.; AlHagar, O.E.A.; Hassan, M.A. Optimization, purification, and biochemical characterization of thermoalkaliphilic lipase from a novel *Geobacillus stearothermophilus* FMR12 for detergent formulations. *Int. J. Biol. Macromol.* **2021**, *181*, 125–135. [CrossRef] [PubMed]
18. Wen, X.; Zhang, B.; Wu, B.; Xiao, H.; Li, Z.; Li, R.; Xu, X.; Li, T. Signaling pathways in obesity: Mechanisms and therapeutic interventions. *Signal Transduct. Target. Ther.* **2022**, *7*, 298. [CrossRef] [PubMed]
19. Kim, D.H.; Park, Y.H.; Lee, J.S.; Jeong, H.I.; Lee, K.W.; Kang, T.H. Anti-Obesity Effect of DKB-117 through the Inhibition of Pancreatic Lipase and α-Amylase Activity. *Nutrients* **2020**, *12*, 3053. [CrossRef] [PubMed]
20. Leandro, A.; Pereira, L.; Gonçalves, A.M.M. Diverse Applications of Marine Macroalgae. *Mar. Drugs* **2020**, *18*, 17. [CrossRef]

21. Daniotti, S.; Re, I. Marine Biotechnology: Challenges and Development Market Trends for the Enhancement of Biotic Resources in Industrial Pharmaceutical and Food Applications. A Statistical Analysis of Scientific Literature and Business Models. *Mar. Drugs* **2021**, *19*, 61. [CrossRef]

22. Sudhakar, K.; Mamat, R.; Samykano, M.; Azmi, W.H.; Ishak, W.F.W.; Yusaf, T. An overview of marine macroalgae as bioresource. *Renew. Sustain. Energy Rev.* **2018**, *91*, 165–179. [CrossRef]

23. Carpena, M.; Garcia-Perez, P.; Garcia-Oliveira, P.; Chamorro, F.; Otero, P.; Lourenço-Lopes, C.; Cao, H.; Simal-Gandara, J.; Prieto, M.A. Biological properties and potential of compounds extracted from red seaweeds. *Phytochem. Rev.* **2022**, 1–32. [CrossRef] [PubMed]

24. Lakey-Beitia, J.; Burillo, A.M.; La Penna, G.; Hegde, M.L.; Rao, K.S. Polyphenols as Potential Metal Chelation Compounds Against Alzheimer's Disease. *J. Alzheimer's Dis.* **2021**, *82*, S335–S357. [CrossRef]

25. Shreadah, M.; Abdel-El Moneam, N.; Al-Assar, S.; Nabil-Adam, A. The ameliorative role of a marine sponge extract against mixture of persistent organic pollutants induced changes in hematological parameters in mice. *Expert Opin. Env. Biol.* **2017**, *6*, 2. [CrossRef]

26. Abdel Moneam, N.; Al-Assar, S.; Shreadah, M.; Nabil-Adam, A. The hepatoprotective effect of *Hyrtios aff. Erectus* sponge isolated from the Red sea extract against the toxicity of Persistent organic pollutants (POPs) from Sediments of Lake Mariout. *J. Biotechnol. Biotechnol. Equip.* **2017**, *32*, 734–743. [CrossRef]

27. Shreadah, M.A.; El Moneam, N.M.A.; Al-Assar, S.A.; Nabil-Adam, A. Phytochemical and pharmacological screening of *Sargassium vulgare* from Suez Canal, Egypt. *Food Sci. Biotechnol.* **2018**, *27*, 963–979. [CrossRef]

28. Cotas, J.; Leandro, A.; Monteiro, P.; Pacheco, D.; Figueirinha, A.; Gonçalves, A.M.M.; da Silva, G.J.; Pereira, L. Seaweed Phenolics: From Extraction to Applications. *Mar. Drugs* **2020**, *18*, 384. [CrossRef]

29. Lomartire, S.; Cotas, J.; Pacheco, D.; Marques, J.C.; Pereira, L.; Gonçalves, A.M.M. Environmental Impact on Seaweed Phenolic Production and Activity: An Important Step for Compound Exploitation. *Mar. Drugs* **2021**, *19*, 245. [CrossRef]

30. Abd El Moneam, N.M.; Shreadah, M.A.; El-Assar, S.A.; De Voogd, N.J.; Nabil-Adam, A. Hepatoprotective effect of Red Sea sponge extract against the toxicity of a real-life mixture of persistent organic pollutants. *Biotechnol. Biotechnol. Equip.* **2018**, *32*, 734–743. [CrossRef]

31. Sęczyk, Ł.; Świeca, M.; Kapusta, I.; Gawlik-Dziki, U. Protein–Phenolic Interactions as a Factor Affecting the Physicochemical Properties of White Bean Proteins. *Molecules* **2019**, *24*, 408. [CrossRef]

32. Wojtunik-Kulesza, K.; Oniszczuk, A.; Oniszczuk, T.; Combrzyński, M.; Nowakowska, D.; Matwijczuk, A. Influence of In Vitro Digestion on Composition, Bioaccessibility and Antioxidant Activity of Food Polyphenols—A Non-Systematic Review. *Nutrients* **2020**, *12*, 1401. [CrossRef]

33. Susmitha, A.; Bajaj, H.; Madhavan Nampoothiri, K. The divergent roles of sortase in the biology of Gram-positive bacteria. *Cell Surf.* **2021**, *7*, 100055. [CrossRef]

34. Nguyen, T.L.A.; Bhattacharya, D. Antimicrobial Activity of Quercetin: An Approach to Its Mechanistic Principle. *Molecules* **2022**, *27*, 2494. [CrossRef] [PubMed]

35. Makarewicz, M.; Drożdż, I.; Tarko, T.; Duda-Chodak, A. The Interactions between Polyphenols and Microorganisms, Especially Gut Microbiota. *Antioxidants* **2021**, *10*, 188. [CrossRef]

36. Lou, Z.; Wang, H.; Rao, S.; Sun, J.; Ma, C.; Li, J. p-Coumaric acid kills bacteria through dual damage mechanisms. *Food Control* **2012**, *25*, 550–554. [CrossRef]

37. Wang, H.; Chu, W.; Ye, C.; Gaeta, B.; Tao, H.; Wang, M.; Qiu, Z. Chlorogenic acid attenuates virulence factors and pathogenicity of *Pseudomonas aeruginosa* by regulating quorum sensing. *Appl. Microbiol. Biotechnol.* **2019**, *103*, 903–915. [CrossRef] [PubMed]

38. Su, M.; Liu, F.; Luo, Z.; Wu, H.; Zhang, X.; Wang, D.; Zhu, Y.; Sun, Z.; Xu, W.; Miao, Y. The Antibacterial Activity and Mechanism of Chlorogenic Acid Against Foodborne Pathogen *Pseudomonas aeruginosa*. *Foodborne Pathog. Dis.* **2019**, *16*, 823–830. [CrossRef]

39. Mu, Y.; Zeng, H.; Chen, W. Quercetin Inhibits Biofilm Formation by Decreasing the Production of EPS and Altering the Composition of EPS in *Staphylococcus epidermidis*. *Front. Microbiol.* **2021**, *12*, 631058. [CrossRef]

40. Vipin, C.; Saptami, K.; Fida, F.; Mujeeburahiman, M.; Rao, S.S.; Athmika; Arun, A.B.; Rekha, P.D. Potential synergistic activity of quercetin with antibiotics against multidrug-resistant clinical strains of *Pseudomonas aeruginosa*. *PloS ONE* **2020**, *15*, e0241304. [CrossRef]

41. Al Azzaz, J.; Al Tarraf, A.; Heumann, A.; Da Silva Barreira, D.; Laurent, J.; Assifaoui, A.; Rieu, A.; Guzzo, J.; Lapaquette, P. Resveratrol Favors Adhesion and Biofilm Formation of *Lacticaseibacillus paracasei* subsp. *paracasei* Strain ATCC334. *Int. J. Mol. Sci.* **2020**, *21*, 5423. [CrossRef]

42. Kato, E.; Tsuruma, A.; Amishima, A.; Satoh, H. Proteinous pancreatic lipase inhibitor is responsible for the antiobesity effect of young barley (*Hordeum vulgare* L.) leaf extract. *Biosci. Biotechnol. Biochem.* **2021**, *85*, 1885–1889. [CrossRef] [PubMed]

43. Oluwagunwa, O.A.; Alashi, A.M.; Aluko, R.E. Inhibition of the in vitro Activities of α-Amylase and Pancreatic Lipase by Aqueous Extracts of *Amaranthus viridis*, *Solanum macrocarpon* and *Telfairia occidentalis* Leaves. *Front. Nutr.* **2021**, *8*, 772903. [CrossRef]

44. Oboh, G.; Ademosun, A.O.; Ayeni, P.O.; Omojokun, O.S.; Bello, F. Comparative effect of quercetin and rutin on α-amylase, α-glucosidase, and some pro-oxidant-induced lipid peroxidation in rat pancreas. *Comp. Clin. Pathol.* **2015**, *24*, 1103–1110. [CrossRef]

45. Zhu, W.; Jia, Y.; Peng, J.; Li, C.-M. Inhibitory Effect of Persimmon Tannin on Pancreatic Lipase and the Underlying Mechanism in Vitro. *J. Agric. Food Chem.* **2018**, *66*, 6013–6021. [CrossRef]

46. Swilam, N.; Nawwar, M.A.M.; Radwan, R.A.; Mostafa, E.S. Antidiabetic Activity and In Silico Molecular Docking of Polyphenols from *Ammannia baccifera* L. subsp. *Aegyptiaca* (Willd.) Koehne Waste: Structure Elucidation of Undescribed Acylated Flavonol Diglucoside. *Plants* **2022**, *11*, 452. [CrossRef]

47. Baruah, I.; Kashyap, C.; Guha, A.K.; Borgohain, G. Insights into the Interaction between Polyphenols and β-Lactoglobulin through Molecular Docking, MD Simulation, and QM/MM Approaches. *ACS Omega* **2022**, *7*, 23083–23095. [CrossRef]

48. Zhang, R.; Wei, Y.; Yang, T.; Huang, X.; Zhou, J.; Yang, C.; Zhou, J.; Liu, Y.; Shi, S. Inhibitory effects of quercetin and its major metabolite quercetin-3-O-β-D-glucoside on human UDP-glucuronosyltransferase 1A isoforms by liquid chromatography-tandem mass spectrometry. *Exp. Ther. Med.* **2021**, *22*, 842. [CrossRef]

49. Ullah, A.; Munir, S.; Badshah, S.L.; Khan, N.; Ghani, L.; Poulson, B.G.; Emwas, A.-H.; Jaremko, M. Important Flavonoids and Their Role as a Therapeutic Agent. *Molecules* **2020**, *25*, 5243. [CrossRef]

50. Cosme, P.; Rodríguez, A.B.; Espino, J.; Garrido, M. Plant Phenolics: Bioavailability as a Key Determinant of Their Potential Health-Promoting Applications. *Antioxidants* **2020**, *9*, 1263. [CrossRef] [PubMed]

51. Chakraborty, K.; Paulraj, R. Sesquiterpenoids with free-radical-scavenging properties from marine macroalga *Ulva fasciata* Delile. *Food Chem.* **2010**, *122*, 31–41. [CrossRef]

52. Tamer, T.M.; Sabet, M.M.; Alhalili, Z.A.H.; Ismail, A.M.; Mohy-Eldin, M.S.; Hassan, M.A. Influence of Cedar Essential Oil on Physical and Biological Properties of Hemostatic, Antibacterial, and Antioxidant Polyvinyl Alcohol/Cedar Oil/Kaolin Composite Hydrogels. *Pharmaceutics* **2022**, *14*, 2649. [CrossRef]

53. Prieto, P.; Pineda, M.; Aguilar, M. Spectrophotometric Quantitation of Antioxidant Capacity through the Formation of a Phosphomolybdenum Complex: Specific Application to the Determination of Vitamin E. *Anal. Biochem.* **1999**, *269*, 337–341. [CrossRef] [PubMed]

54. Garratt, D.C. The Quantitative Analysis of Drugs. In *The Quantitative Analysis of Drugs*; Garratt, D.C., Ed.; Springer US: Boston, MA, USA, 1964; pp. 1–669.

55. El-Samad, L.M.; Hassan, M.A.; Basha, A.A.; El-Ashram, S.; Radwan, E.H.; Abdul Aziz, K.K.; Tamer, T.M.; Augustyniak, M.; El Wakil, A. Carboxymethyl cellulose/sericin-based hydrogels with intrinsic antibacterial, antioxidant, and anti-inflammatory properties promote re-epithelization of diabetic wounds in rats. *Int. J. Pharm.* **2022**, *629*, 122328. [CrossRef]

56. Hassan, M.A.; Abd El-Aziz, S.; Elbadry, H.M.; El-Aassar, S.A.; Tamer, T.M. Prevalence, antimicrobial resistance profile, and characterization of multi-drug resistant bacteria from various infected wounds in North Egypt. *Saudi J. Biol. Sci.* **2022**, *29*, 2978–2988. [CrossRef] [PubMed]

57. Miller, G.L. Use of dinitrosalicylic acid reagent for determination of reducing sugar. *Anal. Chem.* **1959**, *31*, 426–428. [CrossRef]

58. Choi, S.-J.; Hwang, J.-M.; Kim, S.-I. A colorimetric microplate assay method for high throughput analysis of lipase activity. *BMB Rep.* **2003**, *36*, 417–420. [CrossRef] [PubMed]

59. O'Boyle, N.M.; Banck, M.; James, C.A.; Morley, C.; Vandermeersch, T.; Hutchison, G.R. Open Babel: An open chemical toolbox. *J. Cheminformatics* **2011**, *3*, 33. [CrossRef]

60. Daina, A.; Michielin, O.; Zoete, V. SwissADME: A free web tool to evaluate pharmacokinetics, drug-likeness and medicinal chemistry friendliness of small molecules. *Sci. Rep.* **2017**, *7*, 42717. [CrossRef]

61. Mbarik, M.; Poirier, S.J.; Doiron, J.; Selka, A.; Barnett, D.A.; Cormier, M.; Touaibia, M.; Surette, M.E. Phenolic acid phenethylesters and their corresponding ketones: Inhibition of 5-lipoxygenase and stability in human blood and HepaRG cells. *Pharmacol. Res. Perspect.* **2019**, *7*, e00524. [CrossRef]